# Detection and Identification of Intermediates in the Reaction of L-Serine with *Escherichia coli* Tryptophan Synthase via Rapid-Scanning Ultraviolet–Visible Spectroscopy

William Frederick Drewe, Jr., and Michael F. Dunn*

*Department of Biochemistry, University of California, Riverside, California 92521*

*Received October 23, 1984; Revised Manuscript Received February 8, 1985*

ABSTRACT: Rapid-scanning stopped-flow (RSSF) UV–visible spectroscopy has been used to investigate the UV–visible absorption changes (300–550 nm) that occur in the spectrum of enzyme-bound pyridoxal 5′-phosphate during the reaction of L-serine with the $\alpha_2\beta_2$ and $\beta_2$ forms of *Escherichia coli* tryptophan synthase. In agreement with previous kinetic studies [Lane, A., & Kirschner, K. (1983) *Eur. J. Biochem. 129*, 561–570], the reaction with $\alpha_2\beta_2$ was found to occur in three detectable relaxations ($1/\tau_1 > 1/\tau_2 > 1/\tau_3$). The RSSF data reveal that during $\tau_1$, the internal aldimine, E(PLP), with $\lambda_{max} = 412$ nm (pH 7.8), undergoes rapid conversion to two transient species, one with $\lambda_{max} \simeq 420$ nm and one with $\lambda_{max} \simeq 460$ nm. These species decay in a biphasic process ($1/\tau_2$, $1/\tau_3$) to a complicated final spectrum with $\lambda_{max} \simeq 350$ nm and with a broad envelope of absorbance extending out to approximately 525 nm. Analysis of the time-resolved spectra establishes that the spectral changes in $\tau_2$ are nearly identical with the spectral changes in $\tau_3$. Kinetic isotope effects due to substitution of $^2H$ for the $\alpha$-$^1H$ of serine were found to increase the amount of the 420-nm transient and to decrease the amount of the species with $\lambda_{max} \simeq 460$ nm. These findings identify the serine Schiff base (the external aldimine) as the 420 nm absorbing, highly fluorescent transient; the species with $\lambda_{max} \simeq 460$ nm is the delocalized carbanion (quinoidal) species derived from abstraction of the $\alpha$ proton from the external aldimine. The reaction of L-serine with $\beta_2$ consists of two relaxations ($1/\tau_{1\beta} > 1/\tau_{2\beta}$) and yields a quasi-stable species with $\lambda_{max} = 420$ nm, in good agreement with a previous report [Miles, E. W., Hatanaka, M., & Crawford, I. P. (1968) *Biochemistry 7*, 2742–2753]. Analysis of the RSSF spectra indicates that the same spectral change occurs in each phase of the reaction. The similarity of the spectral changes that occur in $\tau_2$ and $\tau_3$ of the $\alpha_2\beta_2$ reaction is postulated to originate from the existence of two (slowly) interconverting forms of the enzyme. A similar explanation is proposed to explain the biphasic character of the reaction of $\beta_2$ with L-serine. It is proposed that the spectrum of the product of the L-serine reaction with $\alpha_2\beta_2$ contains contributions from the Schiff base of the reactive $\alpha$-aminoacrylate species, the external aldimine, and the quinoidal species, all in rapid equilibrium.

The enzyme *Escherichia coli* tryptophan synthase catalyzes the synthesis of tryptophan (Miles, 1979; Yanofsky & Crawford, 1970). The physiologically important synthetic path involves the reactants 3-indole-*d*-glycerol 3′-phosphate (IGP) and L-serine (Scheme I). Indole can be used in place of IGP. The native enzyme is a bienzyme complex with subunit composition $\alpha_2\beta_2$. The $\alpha$ subunits have been shown to catalyze the conversion of IGP to indole and *d*-glyceraldehyde 3-phosphate. The $\beta$ subunits contain tightly bound pyridoxal phosphate (in the form of a lysine Schiff base) and have been shown to catalyze the reaction of indole with serine to yield tryptophan and a water molecule.

Both at the level of subunit function and at the level of the chemical transformations, the $\alpha_2\beta_2$ complex provides a very interesting system for the investigation of enzyme catalysis. The works of Yanofsky, Crawford, Miles, Hammes, York, Kirschner, and their colleagues have found evidence for the existence of cooperative subunit interactions and heterotropic site–site interactions between the $\alpha$ and $\beta$ subunits. The catalytic transformation is potentially an extremely rich source of chemical detail. The overall conversion of IGP and serine to tryptophan and water at the minimum must involve both the formation and the scission of the following bond types: C–C, C–H, C–N, C–O, N–H, and O–H (viz., Scheme I). These transformations are most reasonably interpreted to occur via the catalytic action of acidic and basic groups at the two types of active sites. In addition, the PLP[1] moiety plays a critical role in the catalytic function of the $\beta$ subunit as an electrophilic catalytic group in the activation of L-serine for reaction with indole. The tryptophan synthase system takes on additional interest and significance from the fact that, as an enzyme derived from the intensely investigated *E. coli* tryptophan operon, there are available a wide variety of interesting mutant enzyme species with altered catalytic activities and allosteric properties.

For those processes catalyzed by the $\beta$ subunits, the distinctive UV–visible spectral properties of the PLP moiety allow easy detection of intermediates along the reaction path. The rapid kinetic studies of York, Hammes, Miles, Kirschner, and their colleagues (York, 1970, 1972; Goldberg et al., 1968; Goldberg & Baldwin, 1967; Faeder & Hammes, 1970, 1971; Miles et al., 1968; Lane & Kirschner, 1981, 1983a,b) have shown that the formation of tryptophan from L-serine and

[1] Abbreviations: PLP, pyridoxal 5′-phosphate; $\alpha_2\beta_2$ and $\beta_2$, the native and $\beta_2$ forms of *E. coli* tryptophan synthase (EC 4.2.1.20), respectively; E and E*, enzyme forms distinguished by differences in reactivity toward substrates; E(Ain), the internal $\epsilon$-imino lysyl aldimine form of enzyme-bound PLP; E(S), the enzyme–serine Michaelis complex; E($Aex_1$) and E($Aex_2$), the external aldimines formed respectively with L-serine and L-tryptophan; E($T_1$) and E($T_2$), the tetrahedral intermediates formed respectively in the reactions of L-serine and L-tryptophan with the internal aldimine form of enzyme-bound PLP; E($Q_1$), E($Q_2$), and E($Q_3$), quinoidal species formed along the reaction path; E(A-A), the enzyme-bound $\alpha$-aminoacrylate Schiff base with PLP; EDTA, ethylenediaminetetraacetate; RSSF, rapid-scanning stopped flow.

0006-2960/85/0424-3977$01.50/0 

Scheme I[a]

Catalysis at the Active Sites of the α Subunits

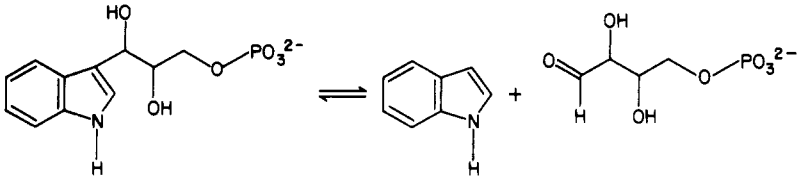


Catalysis at the Active Sites of the β Subunits

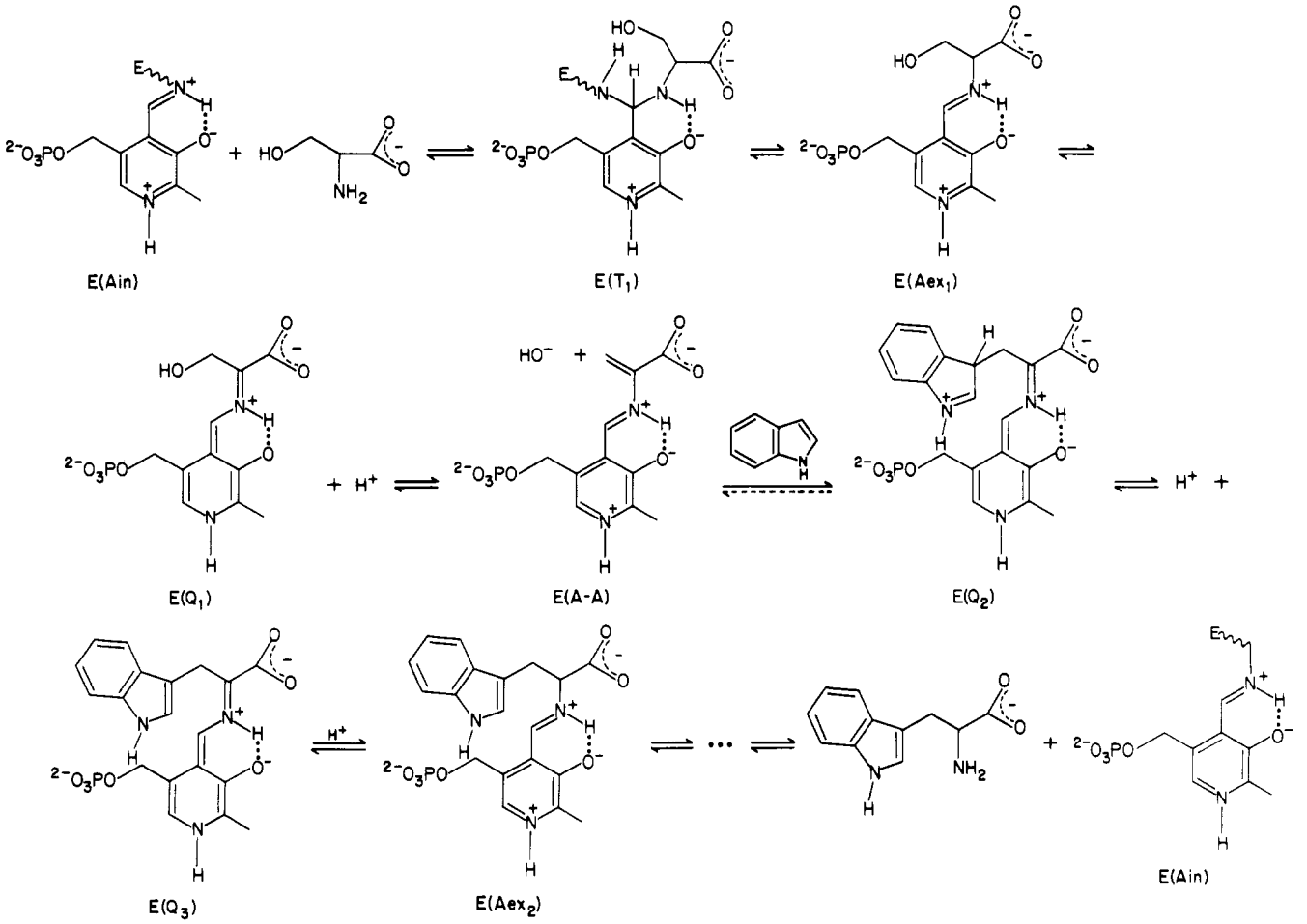


[a] Note that although the protonation state of the PLP chromophore may be different at various steps in catalysis, for simplicity only a single protonation state is shown for each step in this scheme.

indole is a complex multistep process involving several kinetically and spectroscopically detectable intermediates. These previous stopped-flow, rapid-mixing, and temperature perturbation of equilibrium studies have (of necessity) relied upon single-wavelength measurements. In many instances, the kinetic work has been carried out through detection of fluorescence changes (with excitation at a single wavelength) associated with the PLP chromophore. While these studies have contributed substantially to our understanding of the kinetic complexity of the chemical transformations, a detailed analysis of the changes in the UV–visible absorption spectrum that accompany the formation and decay of these intermediates has not yet been presented.

Accordingly, we have initiated detailed investigations of the catalytic mechanism by using rapid-scanning UV–visible spectroscopy in combination with a rapid-mixing stopped-flow apparatus. In this initial account of our studies, we investigate the partial reactions of L-serine with the native $\alpha_2\beta_2$ complex and with the $\beta_2$ dimer. In subsequent papers, we will investigate the pre-steady-state phases of the reaction of indole and L-serine with the native $\alpha_2\beta_2$ complex under different premixing conditions. As will be shown, these studies provide new and more detailed information about the spectral and kinetic properties of the intermediates involved in these reactions. Largely due to advances in the technology used, these studies reveal that additional, heretofore unsuspected, intermediates are formed in these reactions.

## Materials and Methods

Ammonium sulfate (enzyme grade) was purchased from Schwarz/Mann. Sepharose CL-4B was purchased from Pharmacia. All other reagent-grade chemicals were purchased from Sigma and were used without further purification. Buffer solutions were prepared by using doubly glass-distilled water. Enzymatic activity and protein concentration were determined as described by Miles & Moriguchi (1977). DL-[α-$^2$H]Serine was prepared by the method of Miles &McPhie (1974). *E. coli* W3110 tryR$^-$ΔtryLD102/FΔtryLD102 (generously provided by Dr. C. Yanofsky) was grown at 37 °C to early stationary phase in a media composed of 0.05% acid-hydrolyzed

Table I: Summary of Rate Constants, Amplitudes, and Isotope Effects for the Reactions of the $\alpha_2\beta_2$ and $\beta_2$ Forms of *E. coli* Tryptophan Synthase with L-Serine and with DL-[$\alpha$-$^1$H]- and DL-[$\alpha$-$^2$H]Serine[a]

| | | | $\alpha_2\beta_2$ *E. coli* tryptophan synthase | | | | | | |
|---|---|---|---|---|---|---|---|---|---|
| [serine] (mM) | λ (nm) abs | λ (nm) fluorescence | $1/\tau_1$ ($s^{-1}$)[b] | $A_1$[b] | $1/\tau_2$ ($s^{-1}$)[b] | $A_2$[b] | $1/\tau_3$ ($s^{-1}$)[b] | $A_3$[b] | $1/\tau_4$ ($s^{-1}$)[f] |
| 40 (L) | 330 | | | | 68 | 0.049[d] | 16.5 | 0.007[d] | 1.2[d] |
| | 382 | | | | 64 | 0.014[e] | | | 0.6[d] |
| | 430 | | | | 69 | 0.205[e] | 13.0 | 0.02[e] | 0.3[e] |
| | 468 | | | | 71 | 0.036[e] | | | 0.4[d] |
| 4.0 (L) | 430 | | | | 65[e] | 0.062[e] | 13.5[e] | 0.039[e] | 0.4[e] |
| 0.4 (L) | 330 | | | | 12.0 | 0.0096[d] | 2.65 | 0.0022[d] | 0.4[d] |
| | 380 | | | | | | | | 0.65[e] |
| | 430 | | | | 14.3 | 0.055[e] | 2.45 | 0.009[e] | 0.30[e] |
| | 454 | | 145 | 0.038[d] | 15.6 | 0.009[e] | 4.25 | 0.0018[e] | 0.35[e] |
| | 460 | | 136 | 0.019[d] | | | | | 0.50[d] |
| 8 (DL-[$^1$H]) | | $\lambda_{ex}$ = 405, $\lambda_{em}$ = 465 | 195 | 2.10[c,d] | 67.0 | 3.47[e] | | | |
| 8 (DL-[$^3$H]) | | $\lambda_{ex}$ = 405, $\lambda_{em}$ > 465 | 137 | 3.09[c,d] | 15.2 | 2.94[e] | | | |

| | | | $\beta_2$ *E. coli* tryptophan synthase | | | |
|---|---|---|---|---|---|---|
| [serine] (mM) | λ (nm) abs | λ (nm) fluorescence | $1/\tau_{1\beta}$[b] | $A_{1\beta}$[b] | $1/\tau_{2\beta}$[b] | $A_{2\beta}$[b] |
| 40 | 430 | | 207 | 0.034[d] | 41 | 0.057[d] |
| 40 | | $\lambda_{ex}$ = 405, $\lambda_{em} \geq$ 465 | 201 | 1.27[d] | 37 | 2.31[d] |

[a] At 25 °C, in 0.1 M pH 7.80 potassium phosphate buffer containing 1 mM EDTA, with 13.3 μM $\alpha_2\beta_2$ or 13.3 μM $\beta_2$. [b] Rate constants and amplitudes were determined via computer analysis using a nonlinear least-squares reiterative algorithm that assumes the reaction time courses are composed of multiple exponential relaxations (Dunn et al., 1979). Amplitudes are given in units of Δabsorbance for the absorbance measurements and in units of ΔV for the fluorescence measurements. [c] These voltage values are the actual maximum voltage increases observed during $1/\tau_1$ as the fluorescent intermediate forms (viz., Figure 5B). [d] Increasing signal amplitude. [e] Decreasing signal amplitude. [f] The amplitudes for $1/\tau_4$ are all relatively small, ≤0.003 ΔAbs.

casein, 0.5% glucose, and 25 mg/L tryptophan in Vogel–Bonner minimal salts (Vogel & Bonner, 1956) at pH 7.0 (Adaci et al., 1974).

*Purification of Tryptophan Synthase.* All purification steps were carried out at 0–4 °C. This purification scheme is a modification combining the procedure of Adachi et al. (1974) with the Sepharose CL-4B column chromatography (final step) of Tschopp & Kirschner (1980). The enzyme was stored as an ammonium sulfate (35 g/100 mL) precipitate at 4 °C. For any experimental use, suitable amounts of the $\alpha_2\beta_2$ form of the enzyme were centrifuged for 20 min at 25000*g*, and the pellet obtained was dissolved in a minimal volume of 0.1 M potassium phosphate buffer, pH 7.80, containing 1 mM EDTA. This enzyme solution then was dialyzed against 2 500-mL volumes of the same buffer overnight. The $\beta_2$ form of the enzyme was prepared according to the procedure of Högberg-Raiband & Goldberg (1977). For experimental use, the $\beta_2$ dimer was treated in the same manner as the $\alpha_2\beta_2$ form of the enzyme. The purities of $\alpha_2\beta_2$ and $\beta_2$ were found to be >95% according to analysis by SDS–PAGE (Laemmli, 1970).

*Static and Kinetic Spectral Measurements.* Routine UV–visible spectral data were obtained with Varian 635 and Hewlett-Packard 8450A spectrophotometers. Single-wavelength transient kinetic studies were performed with a Durrum Model D-110 stopped-flow spectrophotometer (20-mm light path) interfaced for on-line computer data acquisition and analysis. The hardware and software for this system have been described (Dunn et al., 1979). The concentrations reported refer to conditions after mixing.

*Rapid-Scanning Stopped-Flow (RSSF) Spectrophotometry.* The RSSF spectrophotometer used in these studies employed elements of the Durrum D-110 with a Princeton Applied Research (PAR) OMA-2 multichannel analyzer, 1218 controller, and 1214 photodiode array detector. An external time-delay firing circuit (Koerber, 1981) was used to ensure that the temporal events of flow stoppage and the initiation of data acquisition occur close together in time (typically 2–4 ms after flow stopped). The hardware and software for this RSSF system have been described (Koerber et al., 1983).

For the spectra reported herein, the collection of the first scan relative to flow cessation is noted in the figure legends. In Figures 1 and 2, the repetitive scan rate is 8.605 ms with scan delays to give the following pattern of scans. The 2nd through 19th scans were collected at the following intervals after the first: (2) 8.6, (3) 17.2, (4) 25.8, (5) 34.4, (6) 43.0, (7) 51.6, (8) 60.2, (9) 68.8, (10) 77.4, (11) 86.1, (12) 94.7, (13) 129, (14) 164, (15) 207, (16) 336, (17) 465, (18) 1110, and (19) 1970 ms. In Figure 4, the repetitive scan rate is 4.67 ms, and scans were collected at the following intervals after the first: (2) 4.7, (c) 9.3, (4) 14.0, (5) 18.7, (6) 23.4, (7) 28.0, (8) 32.7, (9) 42.0, (10) 51.4, (11) 60.7, (12) 70.1, (13) 107, (14) 154, (15) 247, (16) 387, (17) 761, (18) 1135, and (19) 1980 ms. In a typical experiment, a "100% transmission" reference spectrum (defined as the light transmitted by the buffer solution used) and the diode "dark-current" spectrum are first collected and stored. By use of these stored spectra, the rapid scanning data are converted to absorbance and stored directly on the floppy disc.

The signals from the 1000 pixels used in these studies were grouped and averaged in sets of either four or eight, resulting in a resolution of ±2 nm (at 8.605 ms/scan) and ±4 nm (at 4.67 ms/scan). The software of the OMA-2 allow arithmetic manipulation of the data to yield single-wavelength time courses and difference spectra.

## Results

*Rapid-Scanning Studies of the Reaction of $\alpha_2\beta_2$ with L-Serine.* The absorbance changes that occur during the reaction of $\alpha_2\beta_2$ at high (40 mM) and low (0.4 mM) levels of L-serine as observed by rapid-scanning stopped-flow spectroscopy are presented in Figure 1A–D. As will be shown (viz., the single-wavelength time courses in Figure 1 and Table I), these time courses consist of at least four relaxations. Henceforth, these relaxations are designated $\tau_1$, $\tau_2$, $\tau_3$, and $\tau_4$ in order of decreasing rate. The family of time-dependent spectra for the wavelength region 300–550 nm (Figure 1A) for the reaction with 40 mM L-serine show that during the dead time of the experiment (~5 ms) the optical densities in the 400–525-nm region increase ($\tau_1$). The changes during $\tau_1$ result in a red shift of the $\lambda_{max}$ from 412 (the native enzyme, spectrum 0)

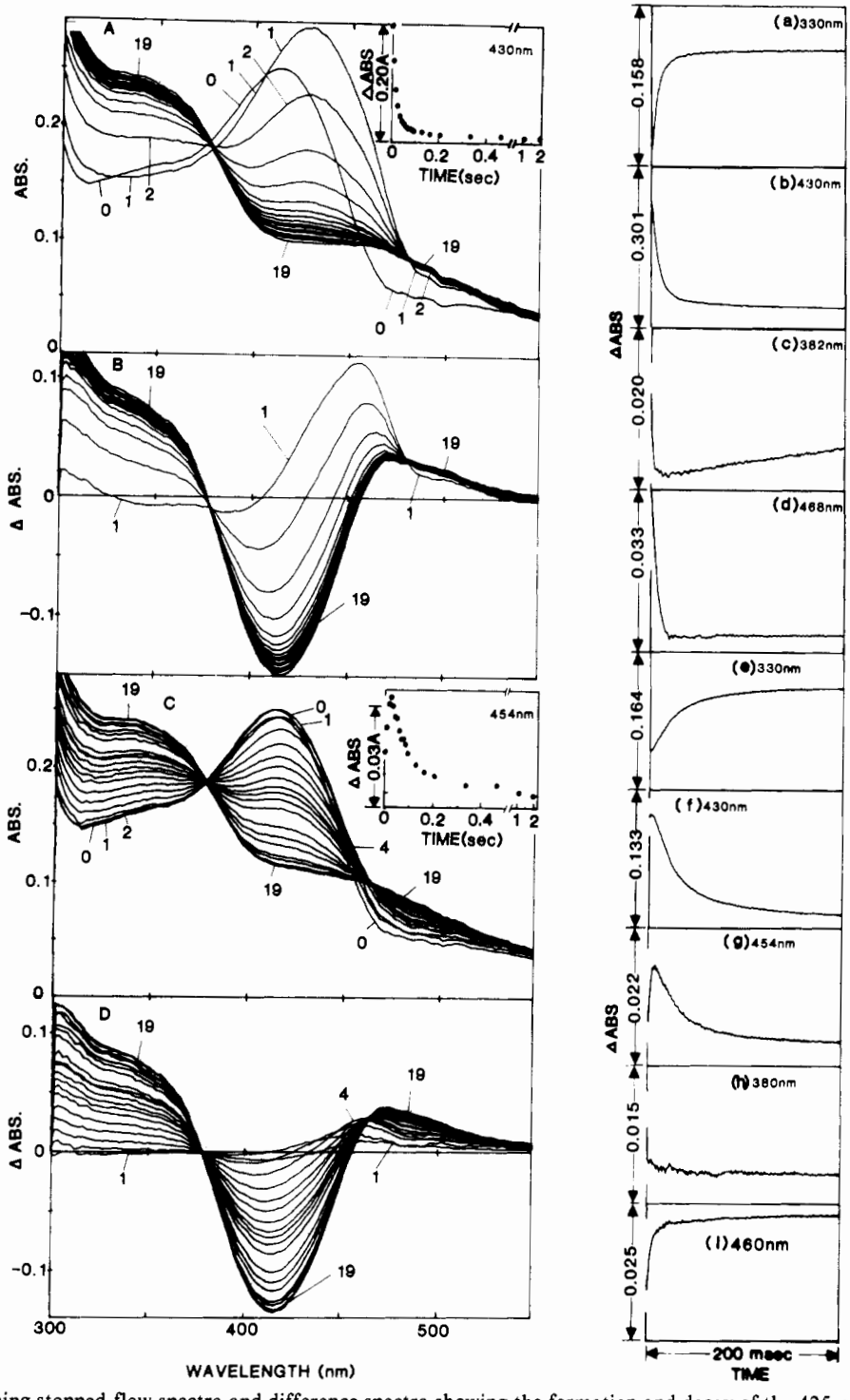


FIGURE 1: Rapid-scanning stopped-flow spectra and difference spectra showing the formation and decay of the 425-nm intermediate and the formation of the pale species for the reaction of the $\alpha_2\beta_2$ enzyme with L-serine. Enzyme spectra A and C and difference spectra B and D were measured respectively at high (40 mM) and low (0.4 mM) concentrations of L-serine. Before mixing, the enzyme was contained in one syringe while L-serine was contained in the other syringe. In (A) and (C), the traces designated 0 are the reconstructed spectra of the reactants. The initiation of scanning in (A) and (C) occurred respectively 1 and 3 ms after flow stopped. See Materials and Methods for the timing sequence. Difference spectra (B) and (D) were computed as $(\text{scan})_t - (\text{scan})_0$ from the data presented in (A) and (C), respectively. The insets are single-wavelength time courses reconstructed from the RSSF data at (A) 430 and (C) 454 nm, respectively. Conditions after mixing: (A and B) [L-Ser] = 40 mM; (C and D) [L-Ser] = 0.4 mM. In each experiment: $[\alpha_2\beta_2]$ = 13.3 $\mu$M, 0.1 M potassium phosphate and 1 mM EDTA, pH 7.80, 25 °C. The conventional stopped-flow time courses (a–i) are for the reaction of the $\alpha_2\beta_2$ enzyme with 40 mM L-serine (a–d) and 0.4 mM L-serine (e–i). Assuming the minimum number of consecutive first-order processes, the best fits of the data are as follows: (330 nm) (a) $1/\tau_2 = 68\ s^{-1}$, $1/\tau_3 = 16.5\ s^{-1}$, and $1/\tau_4 = 1.2\ s^{-1}$; (430 nm) (b) $1/\tau_2 = 69\ s^{-1}$, $1/\tau_3 = 13\ s^{-1}$, and $1/\tau_4 = 0.3\ s^{-1}$; (382 nm) (c) $1/\tau_2 = 64\ s^{-1}$ and $1/\tau_4 = 0.6\ s^{-1}$; (468 nm) (d) $1/\tau_2 = 71\ s^{-1}$ and $1/\tau_4 = 0.4\ s^{-1}$; (330 nm) (e) $1/\tau_2 = 12.0\ s^{-1}$, $1/\tau_3 = 2.65\ s^{-1}$, and $1/\tau_4 = 0.4\ s^{-1}$; (430 nm) (f) $1/\tau_2 = 14.3\ s^{-1}$, $1/\tau_3 = 2.45\ s^{-1}$, and $1/\tau_4 = 0.30\ s^{-1}$; (454 nm) (g) $1/\tau_1 = 145\ s^{-1}$, $1/\tau_2 = 15.6\ s^{-1}$, $1/\tau_3 = 4.25\ s^{-1}$, and $1/\tau_4 = 0.35\ s^{-1}$; (380 nm) (h) $1/\tau_4 = 0.65\ s^{-1}$; (460 nm) (i) $1/\tau_1 = 136\ s^{-1}$ and $1/\tau_4 = 0.5\ s^{-1}$.

to 425 nm (spectrum 1). Following this time-unresolved shift, there is observed an apparent biphasic decrease ($\tau_2$ and $\tau_3$) in optical densities between 380 and 470 nm and a biphasic increase in the 300–380-nm and 470–550-nm regions. The inset to Figure 1A presents the "time slice" taken from the RSSF data at 430 nm and shows both the biphasic decrease

in absorbance and the timing pattern used to gather this family of spectra. As previously reported by York (1970) and by Lane & Kirschner (1983a), the fourth relaxation ($\tau_4$) is characterized by a very small amplitude and a very slow rate (Table I). This relaxation only becomes detectable on time scales >1 s. Because the specific turnover rate $k_{cat} > 5\ s^{-1}$ at pH 7.8 and 25 °C, both groups have considered $\tau_4$ to be irrelevant to catalysis. Accordingly, we also neglect $\tau_4$ in the present study.

In the reaction with 40 mM L-serine (Figure 1A), there appear to be no true isosbestic points; but at 379 nm, there is only a very small deviation from true isosbesty (<0.005 ΔOD). The spectra indicate the existence of two apparent isoabsorptive points during $\tau_3$ located at 383 and 470 nm. During both phases of the decay of this 425-nm species ($\tau_2$ and $\tau_3$), the absorbance decreases at both 383 and 470 nm. The decay of this 425 nm absorbing species during $\tau_2$ and $\tau_3$ is more clearly shown in the difference spectra generated by subtraction of the enzyme spectrum (no. 0) from each of the scans (Figure 1B). These difference spectra show that the optical density changes in each phase, as indicated by the positions of maxima and minima, are nearly identical. Again, it can be seen that as the 425-nm species decays (during $\tau_2$ and $\tau_3$), the optical densities increase both in the wavelength region less than 380 nm and in the region greater than 470 nm.

When a lower level of L-serine is used (4 mM), the appearance ($\tau_1$) of the 425-nm band is slower and can be detected (data not shown); otherwise, the pattern of the spectral changes is quite similar to the pattern shown in Figure 1A (compare Figure 1A with Figure 4A below). Again, there appear to be no isosbestic points. The family of spectra do indicate the existence of two apparent isoabsorptive points during the last observed phase ($\tau_3$) at 380 and 470 nm. During the fastest phase ($\tau_2$) of the decay of the 425-nm species, the absorbance decreases at both 380 and 470 nm.

At the lowest level of L-serine used (0.4 mM), the formation of the transient 425-nm band is not as apparent as with the higher concentrations of L-serine. However, at certain characteristic wavelengths, the optical density changes are triphasic. The time slice at 454 nm (the inset to Figure 1C) and the single-wavelength time course (trace g) clearly show this triphasicity; again, as found with the higher level (4 mM) of L-serine, there first occurs an increase ($\tau_1$) followed by a biphasic decrease in optical density ($\tau_2$ and $\tau_3$). This triphasicity is found in the 410–460-nm region (Figure 1C,D).

In the regions of 300–380 nm and 460–550 nm (Figure 1C,D), there is a biphasic increase ($\tau_2$ and $\tau_3$) in absorbance while the region between 380 and 410 nm undergoes a biphasic decrease ($\tau_2$ and $\tau_3$). Again, no true isosbestic points were found, but at 380 nm, there is only a very small increase in absorbance. The spectra do indicate one apparent *isoabsorptive point* at 460 nm during $\tau_3$. During the fast increase ($\tau_1$) in absorbance at 454 nm, there is a corresponding increase at 460 nm. The family of difference spectra (Figure 1D) generated by subtraction of the enzyme spectrum (no. 0) from each of the scans more clearly shows the presence of the isoabsorptive point at 460 nm.

*Single-Wavelength Stopped-Flow Studies.* Single-wavelength rapid-mixing experiments carried out under experimental conditions identical with those used in the RSSF studies were undertaken to verify the lack of isosbestic points, to verify the existence of isoabsorptive points, and to gather accurate rate parameters. Traces a–d of Figure 1 show the time courses measured at 330, 430, 382, and 468 nm with high (40 mM)

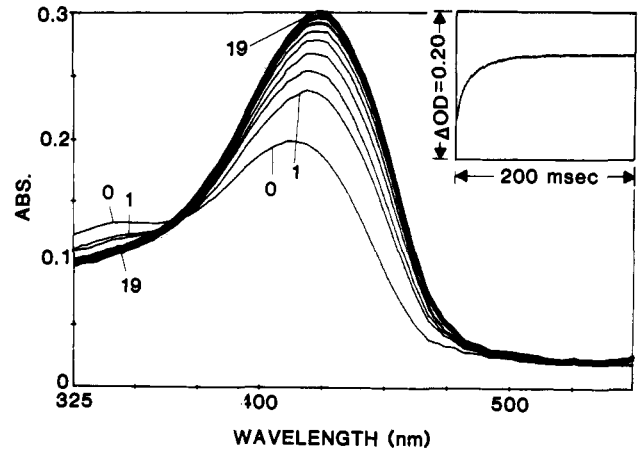


FIGURE 2: Rapid-scanning stopped-flow spectra showing the formation of the aqua (420-nm) species during the reaction of the $\beta_2$ enzyme with L-serine. Trace 0 is the reconstructed spectrum of the reactants. The initiation of scanning occurred 2 ms after flow stopped. Conditions after mixing: [L-serine] = 40 mM; [$\beta_2$] = 13.3 μM, 0.1 M potassium phosphate buffer and 1 mM EDTA, pH 7.80; 25 °C. The inset is a conventional stopped-flow time course measured at 430 nm on mixing the $\beta_2$ enzyme with 40 mM L-serine. See Materials and Methods for the timing sequence.

L-serine. The absorbance at 430 nm increases within the instrument dead time (assumed to consist of a single relaxation, $\tau_1$) and then decreases in three distinct steps according to the expression

$$\Delta A_t = A_1 \exp(-t/\tau_1) - A_2 \exp(-t/\tau_2) - A_3 \exp(-t/\tau_3) - A_4 \exp(-t/\tau_4) \quad (1)$$

where $1/\tau_1$ is the apparent first-order rate constant for the absorbance increase at 430 nm and $1/\tau_2$, $1/\tau_3$, and $1/\tau_4$ are the apparent first-order rate constants for the decrease at 430 nm. $A_1$, $A_2$, $A_3$, and $A_4$ are the reaction amplitudes in the four phases. Only the first three consecutive first-order processes are necessary to accurately describe the time courses (of 2-s duration) at 430 (trace b) and 330 nm (trace a). Within the limits of experimental error (±15%), the measured rates and relative amplitude changes at both wavelengths are the same. At 382 and 468 nm (traces c and d), only the $\tau_2$ and $\tau_4$ processes make significant contributions to the time courses. As indicated in the RSSF spectra (viz., Figure 1A), these time courses verify the existence of apparent isoabsorptive points during $\tau_3$.

Traces e–i of Figure 1 show the single-wavelength time courses for the reaction of $\alpha_2\beta_2$ with the low concentration of L-serine (0.4 mM). Again, at 330 (trace e) and 430 nm (trace f), the measured time courses are triphasic and, within the limits of experimental error, give identical computer-fitted rates and relative amplitude changes. In addition to the triphasic decrease in absorbance at 430 nm, a fourth, faster phase (an absorbance increase) is found at 454 nm (trace g). This absorbance change occurs on the same time scale as the increase in absorbance ($\tau_1$) that occurs in the dead time for the reaction with high (40 mM) L-serine. At 380 nm (trace h) only the $\tau_4$ process (an absorbance increase) is detected while at 460 nm (trace i) both $\tau_1$ and $\tau_4$ were observed.

*Rapid-Scanning Studies of the Reaction of $\beta_2$ with L-Serine.* The reaction of the $\beta_2$ form of the enzyme with 40 mM L-serine was also studied (Figure 2). Reaction has been shown to result in the rapid formation of a quasi-stable species with $\lambda_{max}$ = 420 nm (Goldberg et al., 1968), which slowly turns over yielding pyruvate, $NH_3$, and $H_2O$. The set of scans shown in Figure 2 correspond to the time interval during which the 420-nm species forms. These scans indicate an increase in

absorbance at wavelengths greater than 370 nm, while the absorbance at wavelengths less than 370 nm decreases. Note the similarity of the last spectrum obtained in the $\beta_2$–serine reaction, with $\lambda_{max}$ = 420 nm (spectrum 19, Figure 2), to the first spectrum observed in the $\alpha_2\beta_2$–serine reaction (spectrum 1, Figure 1A). When normalized to the same amplitude scale (Figure 3), comparison of the two bands reveals that the 425-nm band in the first spectrum obtained in the $\alpha_2\beta_2$–serine reaction has a width at half-maximum of $4.86 \times 10^3$ cm$^{-1}$ (86 nm) while the final spectrum in the $\beta_2$–serine reaction has a width at half-maximum of $4.49 \times 10^3$ cm$^{-1}$ (78 nm). Subtraction of the normalized spectra yields a difference spectrum (Figure 3) that has an absorbance maximum of ~460 nm and a half-maximum band width of $1.64 \times 10^3$ cm$^{-1}$ (35 nm). One explanation for the increased band width of the 425-nm transient (spectrum 1 of Figure 1A) is that the absorption envelope includes a longer wavelength band ($\lambda_{max} \simeq 460$ nm) which appears not to be present in the spectrum of the product(s) of the reaction of $\beta_2$ with L-serine.

The time course for the reaction of the $\beta_2$ enzyme with L-serine under conditions identical with those given in the caption of Figure 2 was also measured at 430 nm (see the inset to Figure 2). The absorbance at 430 nm increases in two distinct steps according to the expression

$$\Delta A_t = A_{1\beta} \exp(-t/\tau_{1\beta}) + A_{2\beta} \exp(-t/\tau_{2\beta}) \qquad (2)$$

where $1/\tau_{1\beta}$ and $1/\tau_{2\beta}$ are the apparent first-order rate constants and $A_{1\beta}$ and $A_{2\beta}$ are the amplitudes changes during the two phases.

*Fluorescence Studies.* A highly fluorescent species, the "aqua" species, (Goldberg et al., 1968), is formed by the addition of L-serine to the $\beta_2$ enzyme, and a similar but transient fluorescent intermediate is found in the reaction of L-serine with the $\alpha_2\beta_2$ enzyme (York, 1972; Lane & Kirschner, 1983a). Because the rapid-scanning stopped-flow experiments show the transient appearance of an absorber similar to the highly fluorescent $\beta_2$ "aqua" species, rapid-mixing fluorescence studies were initiated to further characterize this intermediate. In these studies, an excitation wavelength of 405 nm (from a tungsten lamp source) was used, and the total emission passed by a Schott GG-455 filter (50% $T$ at 445 nm) was measured. The fluorescence time course (not shown) in the reaction of $\beta_2$ with L-serine (under conditions identical with those used in Figure 2) was similar in phasicity, fitted rate constants, and relative amplitude changes to the absorbance time course measured at 430 nm (inset to Figure 2). The fluorescence time courses (not shown) in the reaction of $\alpha_2\beta_2$ with high and low L-serine concentrations (under experimental conditions identical with those used in A and E, of Figure 1, respectively) were similar in phasicity, measured rates, and relative amplitude changes to the absorbance time courses at 430 nm (Figure 1, traces b, e and g), except that the $\tau_4$ process was not found.

*Kinetic Isotope Studies with $\alpha$-$^1$H- and $\alpha$-$^2$H-Substituted* DL-*Serine.* The deuterium kinetic isotope studies of Miles & McPhie (1974) (see Discussion) identify the highly fluorescent species formed in the reaction of L-serine with $\beta_2$ as the external aldimine. However, from similar deuterium kinetic isotope studies Lane & Kirschner (1983a) concluded that the fluorescent species formed during $\tau_1$ of the $\alpha_2\beta_2$ reaction probably is the delocalized carbanion (quinoid) species derived from the abstraction of the $\alpha$ proton of the external aldimine. Since the spectra presented in Figures 1 and 2 show that the reactions of L-serine with $\alpha_2\beta_2$ and with $\beta_2$ both yield 420–425 nm absorbing species (Figure 3) with similar fluorescent properties, it seemed unlikely to us that these spectral bands

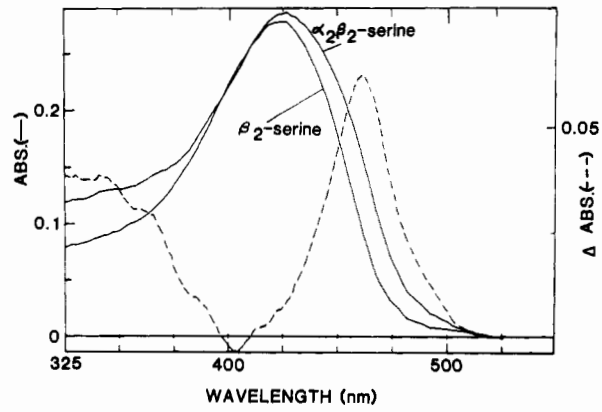


FIGURE 3: Normalized spectra (—) and difference spectrum (- -) comparing the 425-nm $\alpha_2\beta_2$ transient species with the quasi-stable 420-nm $\beta_2$ species formed in the L-serine reactions. The trace labeled $\beta_2$–serine is the 19th spectrum from Figure 2 (the $\beta_2$–L-serine species). The trace-labeled $\alpha_2\beta_2$–serine is the first spectrum from Figure 1A (the $\alpha_2\beta_2$–L-serine transient species). These spectra were base-line zeroed and normalized by adjusting each spectrum to the same amplitude. The difference spectrum was generated by subtracting the normalized $\beta_2$–serine final spectrum from the normalized $\alpha_2\beta_2$–serine spectrum.

arise from structurally different species. Consequently, we decided to further investigate the identity of species formed during $\tau_1$ of the $\alpha_2\beta_2$ reaction. Therefore, a detailed investigation of the effects of $^2$H substitution for the $\alpha$-$^1$H of DL-serine upon the spectral changes that occur during the reaction was undertaken. Lane & Kirschner (1983a) reported that the presence of D-serine has no effect upon the kinetics of the reaction of L-serine with $\alpha_2\beta_2$. Thus, for convenience of synthesis, DL-[$\alpha$-$^2$H]serine was prepared for these experiments by the method of Miles & McPhie (1974).

The RSSF data presented in Figure 4 compare the transient spectral changes that occur in the reactions of 8 mM DL-[$\alpha$-$^1$H]serine (Figure 4A) and 8 mM DL-[$\alpha$-$^2$H]serine (Figure 4B) with $\alpha_2\beta_2$. In these experiments, the scan rate is 4.67 ms/scan, and the wavelength resolution is ±4 nm. Comparison of the spectra in Figure 4 indicate that substitution of $^2$H for $^1$H alters the rates and amplitudes of the spectral changes. To allow a more direct comparison of the salient features of these changes, the spectrum corresponding to the maximum amount of the 425-nm transient formed during an equivalent experiment with 80 mM serine is presented in Figure 5A. It is obvious from inspection of Figure 5A that substitution of deuterium results both in a substantial increase in the amplitude of the 425-nm band and in a substantial decrease in the width of the 425-nm band. The kinetic traces presented in Figure 5B compare the effects of deuterium substitution at the $\alpha$ carbon on the rates and amplitudes of the fluorescence time courses for these reactions (with 8 mM DL-[$\alpha$-$^2$H]serine) in the same solutions used to obtain the data for Figure 4. These time courses show that, in agreement with Lane & Kirschner (1983a), the substitution of deuterium significantly reduces the rates of $\tau_1$, $\tau_2$, and $\tau_3$; however, it is of critical importance to note that the (absolute) amplitude of the fluorescent signal is significantly increased.

## DISCUSSION

The time barrier to the study of enzyme-catalyzed transient and pre-steady-state reactions for time scales ≥1 ms has been circumvented by rapid-mixing stopped-flow technology. In principle, time-resolved spectra could be constructed from a set of single-wavelength time courses measured at different wavelengths. However, due to the enormous investment of effort and/or resources required, most studies have been re-

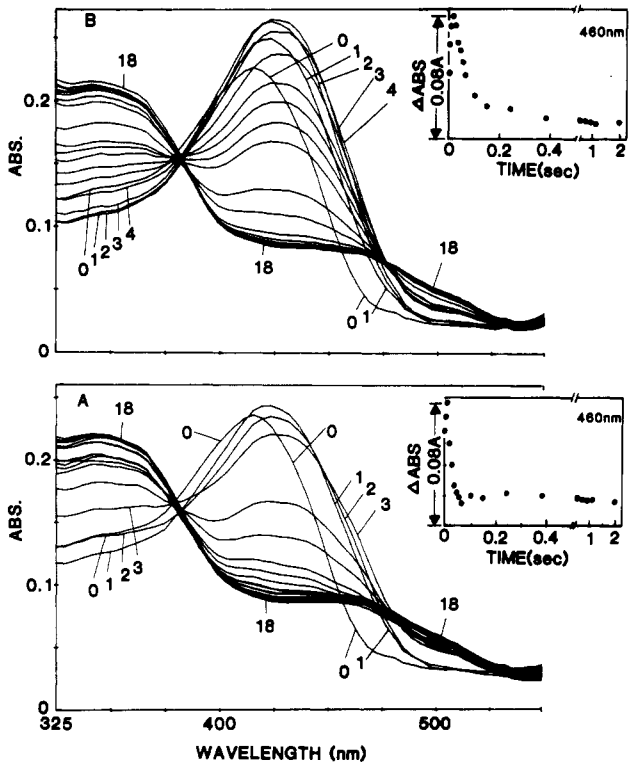


FIGURE 4: Rapid-scanning stopped-flow data comparing the effects of deuterium substitution for the $\alpha$-hydrogen of DL-serine upon the spectra of transient species formed during the reaction of $\alpha_2\beta_2$ with serine. The trace designated 0 is the reconstructed spectrum of the reactants. The initiation of scanning in both (A) and (B) occurred 2 ms after flow stopped. The insets to both (A) and (B) are 460-nm reaction time courses reconstructed from the RSSF data. Conditions after mixing: (A) 8 mM DL-[$\alpha$-$^1$H]serine; (B) 8 mM DL-[$\alpha$-$^2$H]serine. In each experiment: $[\alpha_2\beta_2]$ = 13.3 $\mu$M; 0.1 M potassium phosphate and 1 mM EDTA, pH 7.80; 25 °C. See Materials and Methods for the timing sequence.

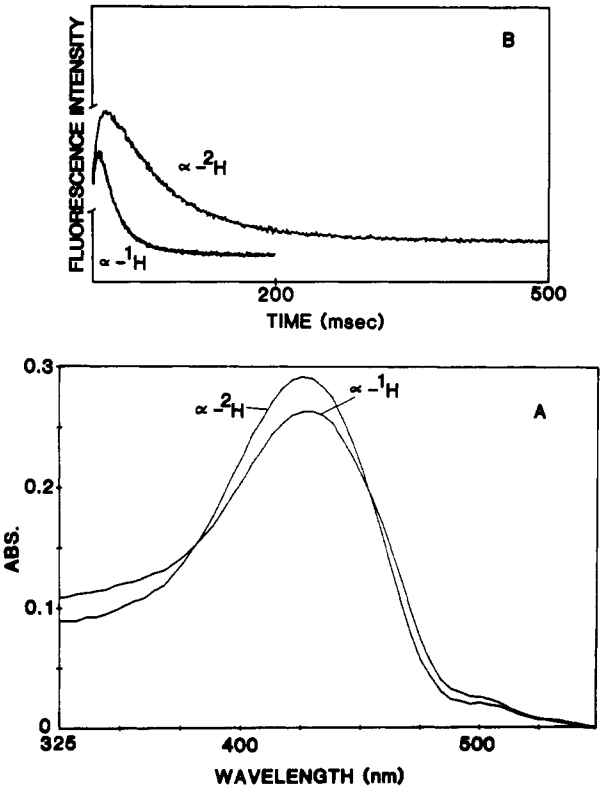


FIGURE 5: Deuterium isotope effects on the time-resolved UV–visible absorbance spectra (A) and fluorescence kinetic time courses (B) for the reaction of $\alpha_2\beta_2$ with DL-[$\alpha$-$^1$H]- and DL-[$\alpha$-$^2$H]serine. The two spectra presented in (A) are taken from RSSF experiments where the DL-[$\alpha$-$^1$H]- and DL-[$\alpha$-$^2$H]serine concentrations were 80 mM. The spectra were both scanned 3 ms after flow stopped. For comparison with the RSSF data in Figure 4, the fluorescent time courses (B) were collected under conditions identical with those described in Figure 4, i.e., with 8 mM DL-serine.

stricted to a few selected wavelengths. Hence, the constraint to measurements at a few wavelengths by conventional single-wavelength instruments greatly restricts the amount of spectral information gathered. Previous rapid kinetic investigations of the tryptophan synthase catalytic mechanism have been subject to such limitation. As is evident in the present work, the application of rapid-scanning, rapid-mixing, UV–visible spectrophotometry to the tryptophan synthase system has allowed us to undertake a more detailed investigation of the spectral changes that occur during the reaction with L-serine. In subsequent papers, we shall present detailed rapid-scanning, stopped-flow studies of the spectral changes that occur during the transient and pre-steady-state phases of the reaction of the enzyme with L-serine and indole and with various substrate analogues.

Heretofore, UV–visible spectroscopic studies of the tryptophan synthase reaction with L-serine have been restricted to the determination of the spectra of reactants and products (viz., spectrum 0 and spectrum 19 of Figure 1A) and to the measurement of single-wavelength absorbance (Faeder & Hammes, 1970, 1971; Goldberg et al., 1967, 1968; Lane & Kirschner, 1983a,b; Miles et al., 1968, 1974, 1977; York, 1972) and fluorescence time courses (Lane & Kirschner, 1983a; York, 1970). The elegant fluorescence work of Lane & Kirschner (1983a) establishes that the time course for the reaction of $\alpha_2\beta_2$ with L-serine consists of at least four detectable relaxations.

The time-resolved spectra and difference spectra and the single-wavelength time courses presented in Figures 1–5 define the nature of the changes that occur in the electronic spectrum of the PLP chromophore as reaction of $\alpha_2\beta_2$ (Figures 1 and 4) or $\beta_2$ (Figure 2) with L-serine ensues. These spectra and our single-wavelength absorption and fluorescence measurements (Figures 1, 2, and 5 and Table I) detect at least four relaxations ($\tau_1$, $\tau_2$, $\tau_3$, and $\tau_4$) in the $\alpha_2\beta_2$ system with apparent rate constants in good agreement with the values reported by Lane & Kirschner (1983a). The $\beta_2$ system yields a time course consisting of two relaxations, $\tau_{1\beta}$ and $\tau_{2\beta}$ (Figure 2 and Table I).

*Analysis of the PLP UV–Visible Spectral Changes during $\tau_1$ of the $\alpha_2\beta_2$ Reaction with L-Serine.* Upon mixing with 40 mM L-serine, the transient changes in the PLP spectrum of the $\alpha_2\beta_2$ species (Figure 1) are characterized by the very rapid formation ($\tau_1$) of a new spectral band with $\lambda_{max} \simeq 425$ nm and with a slight shoulder on the long-wavelength side (Figure 3). The species formed in $\tau_1$ then decays in a biphasic process ($\tau_2$ and $\tau_3$) to a final reaction mixture exhibiting spectral bands at ~350 and 430–450 nm (Figure 1). Due to the small rate constant and amplitude associated with $\tau_4$, we conclude (as previously mentioned) that this process is irrelevant to catalysis.

In contrast to the $\alpha_2\beta_2$ system and in agreement with previous findings (Lane & Kirschner, 1983a; Goldberg et al., 1967; York, 1972), reaction of L-serine with the $\beta_2$ species yields a quasi-stable 420-nm species, and the time course consists of two relaxations ($\tau_{1\beta}$ and $\tau_{2\beta}$, Figure 2). The similarity of this 420-nm species to the first transient species detected in the $\alpha_2\beta_2$ system is striking (compare Figures 1–3). In addition to similar $\lambda_{max}$ and apparent $\epsilon$ values, both species are highly fluorescent (York, 1972; Faeder & Hammes, 1970,

1971; Miles et al., 1968; Goldberg et al., 1968; Lane & Kirschner, 1983a). However, when normalized to the same amplitude (Figure 3), it is apparent that the 425-nm transient detected in the $\alpha_2\beta_2$ reaction has a significantly broader apparent bandwidth (at half-height) than does the 420-nm $\beta_2$ species; the difference between the two spectral envelopes (Figure 3) suggests that the apparent band broadening of the $\alpha_2\beta_2$ transient is due to the presence of an additional, longer wavelength electronic transition ($\lambda_{max} \simeq 460$ nm) that is overlapped and partially obscured by the more intense 420-nm band.

Miles et al. (1968) have shown that the (highly fluorescent) 420-nm $\beta_2$–L-Ser species undergoes a very slow decay reaction to yield pyruvate and ammonium ion (eq 3). The rate of this

$$\beta_2 + \text{L-Ser} \rightleftharpoons^{\text{fast}} \cdots \rightleftharpoons \text{420-nm species} \rightleftharpoons^{\text{very slow}} \cdots \rightarrow \text{CH}_3\text{—C(=O)—C(=O)—O}^- + \text{NH}_4^+ + \beta_2 \quad (3)$$

decay process is subject to a primary kinetic isotope effect ($k_H/k_D = 4$) when L-[$\alpha$-$^2$H]serine is substituted for L-[$\alpha$-$^1$H]serine. Consequently, Miles & McPhie (1974) assigned the 420-nm spectral band to the external aldimine, E(Aex$_1$) of Scheme I. In similar isotope studies but with the $\alpha_2\beta_2$ system, Lane & Kirschner (1983a) found that substitution of $^2$H for the $\alpha$-$^1$H of serine results in a primary isotope effect on $1/\tau_1$ of 2.0 at pH 7.6.

Single-wavelength measurements (Figure 1) indicate that the increases in optical density at 425 nm and at 460 nm both occur with the observed rate, $1/\tau_1$. However, the fast rate of the increase at high concentrations of L-serine and the small amplitude at lower concentrations preclude a rigorous analysis via stopped-flow methods to determine whether or not this process is in fact a single relaxation. If formation of the external aldimine (step $k_3$, $k_{-3}$, Scheme II) and conversion of the aldimine to the quinoidal species (step $k_4$, $k_{-4}$) have comparable activation energies, then $\tau_1$ is determined by at least two coupled steps with similar rates (steps $k_3$, $k_{-3}$, and $k_4$, $k_{-4}$), which are preceded by the rapid formation of E(S) and the first tetrahedral species, E(T$_1$). If scission of the serine $\alpha$-C–H bond occurs in the transition state of step $k_4$, $k_{-4}$, then the initial portion of the reaction time course ($\tau_1$) would be influenced by substitution of $^2$H for the $\alpha$-$^1$H of L-serine.

Scheme II

$$\alpha_2\beta_2 + \text{L-serine} \underset{k_{-1}}{\overset{k_1}{\rightleftharpoons}} \text{E(S)} \underset{k_{-2}}{\overset{k_2}{\rightleftharpoons}} \text{E(T}_1\text{)} \underset{k_{-3}}{\overset{k_3}{\rightleftharpoons}} \text{E(Aex}_1\text{)} \underset{k_{-4}}{\overset{k_4}{\rightleftharpoons}} \text{E(Q}_1\text{)}$$

The deuterium kinetic isotope studies presented in Figures 4 and 5 provide strong evidence in support of this interpretation. The spectra presented in Figures 4 and 5A unambiguously demonstrate that substitution of deuterium for the $\alpha$-hydrogen of serine *alters the relative amounts* of species that accumulate during $\tau_1$. The species with $\lambda_{max} = 420$ nm is increased, while the species with $\lambda_{max} \simeq 460$ nm is decreased. The result is a larger amplitude at 425 nm and a narrower bandwidth. These same amplitude effects are also seen in the fluorescence time courses presented in Figure 5B. *The amplitude of the fluorescence signal is increased* upon substitution of deuterium for the $\alpha$-hydrogen, indicating an increase in the amount of the fluorescent species that accumulates during $\tau_1$. With reference to Scheme I, these data are fully consistent with an increased accumulation of the external aldimine during $\tau_1$, which must be due to the kinetic isotope effect upon the conversion of external aldimine to the quinoidal species. Consequently, these experiments identify the external aldimine, E(Aex$_1$), as the 420 nm absorbing, highly fluorescent transient formed during $\tau_1$, while the species with $\lambda_{max} \simeq 460$ nm must be the quinoidal species, E(Q$_1$).

The amount of quinoid formed in the initial phase of the reaction can be estimated from the following considerations. Assume the 410-nm spectral bands of the internal aldimines of $\alpha_2\beta_2$ and $\beta_2$ have nearly identical extinction coefficients (Lane & Kirschner, 1983a). Under this assumption, then the smaller amplitude of the absorbance increase at 425 nm of the $\alpha_2\beta_2$–L-serine reaction vis a vis the $\beta_2$–L-serine reaction very likely results from the conversion of the external aldimine to the quinoidal intermediate. If the amount of quinoidal species that decays via $1/\tau_2$ during the experiment deadtime (<10 ms) is assumed to be negligible ($1/\tau_2 \leq 70$ s$^{-1}$), then from inspection of Figures 1, 3, and 4 it appears that the external aldimine and the quinoid accumulate during $\tau_1$ in the ratio of at least 3 or 4 to 1 or larger.

*Mechanistic Inferences from the Analysis of $\tau_2$ and $\tau_3$.* The decay processes $\tau_2$ and $\tau_3$ are notable in that the spectral changes in each process are nearly identical (viz., the difference spectra presented in Figure 1B). The final spectrum for the reaction of $\alpha_2\beta_2$ with L-serine (spectrum 19, Figure 1A) appears to consist of several overlapping spectral bands, indicating the presence of several PLP species rather than a single chromophore. We consider it unlikely that the broad envelope of absorbance between 375 and 525 nm could arise from a single PLP species. Since this reaction mixture is highly reactive toward indole, $\beta$-mercaptoethanol, and various other thiols (York, 1970, 1972; Lane & Kirschner, 1983b; Esaki et al., 1983; W. F. Drewe, Jr., and M. F. Dunn, unpublished results) and since reduction with $NaBH_4$ yields (*N*-phosphopyridoxyl)alanine (Miles et al., 1982), the $\alpha$-aminoacrylate, E(A-A) of Scheme I, must be present. If precursors of the $\alpha$-aminoacrylate are also present, then to account for the rapid and nearly quantitative reaction with $\beta$-mercaptoethanol all these species must be assumed to be in rapid equilibration.

For the following reasons, an ~480-nm band is the most probable spectral assignment for the highly reactive form of the $\alpha$-aminoacrylate: (1) the highly conjugated $\alpha$-aminoacrylate aldimine structure is consistent with a 480-nm electronic transition, and (2) the reaction of *O*-acetylserine sulfhydrylase with *O*-acetyl-L-serine in the absence of sulfide ion yields a 470-nm species tentatively identified as the $\alpha$-aminoacrylate (Becker et al., 1969). Their 470-nm species is characterized by a relatively broad bandwidth and a relatively low apparent extinction coefficient ($\epsilon \simeq 8.5 \times 10^3$ M$^{-1}$ cm$^{-1}$). We speculate that the broad absorption envelope between 400 and 475 nm very likely also includes contributions from the external aldimine ($\lambda_{max} = 420$ nm) and the quinoidal species (with $\lambda_{max} \simeq 460$ nm).

The strong spectral band centered at 350 nm could be due to a different form of the $\alpha$-aminoacrylate, i.e., a different tautomer, a different protonation state, or a different conformational isomer. A 480-nm $\alpha$-aminoacrylate species could also have a second electronic transition that contributes to the 350-nm band.

The finding that the spectral changes in $\tau_2$ and $\tau_3$ are nearly identical places new constraints on explanations for the events that take place as the external aldimine and the quinoidal species decay to the aminoacrylate. If $\tau_2$ and $\tau_3$ represented the buildup and decay of an intermediate (N), eq 4, with a

$$\text{M} \underset{k_{-N}}{\overset{k_N}{\rightleftharpoons}} \text{N} \underset{k_{-O}}{\overset{k_O}{\rightleftharpoons}} \text{O} \quad (4)$$

spectrum that is substantially different from both the spectrum

Scheme III

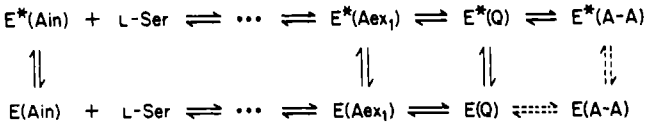


generated in $\tau_1$ (i.e., the spectrum of M) and the final spectrum (the spectrum of O), then the spectral changes that occur in $\tau_2$ would be different from those in $\tau_3$. The analytical expressions[2] for both $\tau_2$ and $\tau_3$ in this reaction as defined for eq 4 (Bernasconi, 1976) would include all four rate constants, $k_N$, $k_{-N}$, $k_O$, and $k_{-O}$. Consequently, we consider it unlikely that $\tau_2$ and $\tau_3$ arise from the formation and decay of a chemical intermediate.

By postulating the existence of two slowly interconverting forms of the $\alpha_2\beta_2$ enzyme (Scheme III), the close similarities of the spectral changes in $\tau_2$ to those in $\tau_3$ can be explained in the following way: During $\tau_1$ both forms react with L-serine at similar rates to form the external aldimine and quinoid species.[3] However, the two forms undergo conversion to the aminoacrylate at different rates, thus giving rise to the two relaxations, $\tau_2$ and $\tau_3$. The observation of a fourth relaxation, $\tau_4$, is not inconsistent with this scheme.

Alternatively, the close similarity of the spectral changes in $\tau_2$ and $\tau_3$ could be explained if the enzyme-bound aminoacrylate intermediate undergoes a conformation change, E-(A-A) ⇌ E*(A-A), with the rate $1/\tau_3$ (Scheme IV). The consequent redistribution of bound species during $\tau_3$ to give a net increase in the amount of bound aminoacrylate with corresponding decreases in the external aldimine and the quinoid would result in nearly identical spectral changes for $\tau_2$ and $\tau_3$.

Scheme IV

$$E(Ain) + L\text{-}Ser \rightleftharpoons \cdots \rightleftharpoons E(Aex_1) \rightleftharpoons E(Q) \rightleftharpoons E(A\text{-}A) \rightleftharpoons E^*(A\text{-}A)$$

Slight differences in the spectra of the two aminoacrylates would account for the highly similar but not identical spectral changes that take place in $\tau_2$ and $\tau_3$. The tight coupling of proton abstraction from the external aldimine with subsequent steps, as depicted in either of these schemes, could account for the isotope effects on $\tau_1$, $\tau_2$, and $\tau_3$ reported by Lane & Kirschner (1983a).

Lane & Kirschner (1981, 1983a,b) have come to slightly different conclusions about the origins of $\tau_2$ and $\tau_3$. While the concentration dependencies of $1/\tau_1$, $1/\tau_2$, and $1/\tau_3$ could be fit to a linear mechanism such as Scheme IV, they concluded that a linear mechanism does not fit the data as well as does the branched mechanism shown in Scheme V. This

Scheme V

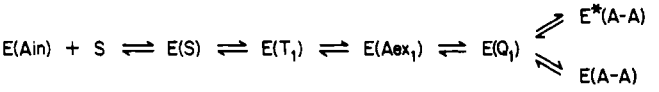


scheme invokes the formation of two catalytically competent $\alpha$-aminoacrylate species via the partitioning of a single quinoid species, one formed at the rate $1/\tau_2$ and the other formed at the rate $1/\tau_3$. These two species are postulated to react at the same rate with indole via this branched pathway, ultimately to form L-tryptophan. According to this mechanism, the primary isotope effects reported for $\tau_2$ and $\tau_3$ are the consequence of a (partially) rate-limiting abstraction of the $\alpha$ proton from the external aldimine in $\tau_1$ that is coupled to $\tau_2$ and $\tau_3$.

The reaction of $\beta_2$ with L-serine to form the external aldimine occurs in two relaxations, $\tau_{1\beta}$ and $\tau_{2\beta}$. The spectra in Figure 2 indicate that the spectral changes in $\tau_{1\beta}$ are essentially identical with the spectral changes in $\tau_{2\beta}$. Just as argued for the $\alpha_2\beta_2$ species, the similarity of these spectral changes indicate the existence of two interconverting forms of the external aldimine $\beta_2^*(Aex_1) \rightleftharpoons \beta_2(Aex_1)$, viz., Scheme VI.

Scheme VI

$$\beta_2^* + L\text{-}Ser \rightleftharpoons \beta^*{}_2(S) \rightleftharpoons \beta^*{}_2(T_1) \rightleftharpoons \beta^*{}_2(Aex_1) \rightleftharpoons \beta_2(Aex_1)$$

*Role of Subunit Interactions in Tryptophan Synthase Catalysis.* Miles & McPhie (1974) have demonstrated that proton abstraction from the $\alpha$ carbon of the external aldimine is a component of the rate-limiting step for the reactions involving the 420-nm $\beta_2$–L-serine species. As already discussed, Lane & Kirschner (1983a) have shown that reaction of $\alpha_2\beta_2$ with L-serine also involves the (partially) rate-determining abstraction of a proton from the external aldimine. As is evident in Figures 1 and 2, and in agreement with the observations of others (Faeder & Hammes, 1970, 1971; Lane & Kirschner, 1983a,b; York, 1970, 1972), the $\alpha$ subunit alters both the rates of chemical steps in the reaction of L-serine with PLP bound to the $\beta$ subunit and the thermodynamic stabilities of bound intermediates along the reaction path. In the absence of indole, the reaction of $\beta_2$ with L-serine (Figure 2) does not yield spectrophotometrically detectable amounts of intermediates along the tryptophan synthetic pathway beyond the external aldimine, $E(Aex_1)$ (viz., Scheme I), whereas the reaction of $\alpha_2\beta_2$ with L-serine yields significant amounts of an aminoacrylate species, E(A-A), which is highly reactive toward indole.

The substrate motions that accompany the change from $sp^3$ to $sp^2$ hybridization at the serine C-$\alpha$ and C-$\beta$ atoms in the conversions of external aldimine to aminoacrylate (viz., Scheme I) very likely occur with obligatory (local) changes in protein conformation. In the $\alpha_2\beta_2$ system, these conformation changes appear to contribute both to a lowering of the activation energies of these steps and to the stabilization of the quinoid and aminoacrylate intermediates. In the $\beta_2$ system, these conformational events appear to be unfavorable thermodynamic processes. Therefore, it appears that the interactions between $\alpha$ and $\beta$ subunits are of critical importance both to the chemical and to the conformational events that occur in the reaction with L-serine.

ACKNOWLEDGMENTS

We thank Professor Charles Yanofsky for his generous gift of the *E. coli* mutant used in the preparation of tryptophan synthase, and we thank Professor William Belser for advice and assistance in the fermentation and culturing of the mutant. We are appreciative of the technical assistance provided by

[2] The general solution to eq 4 for the case where the two steps equilibrate at similar rates gives

$$1/\tau_2 = (1/2)\Sigma k + ([(1/2)\Sigma k]^2 - \Pi k)^{1/2}$$

and

$$1/\tau_3 = (1/2)\Sigma k - ([(1/2)\Sigma k]^2 - \Pi k)^{1/2}$$

where

$$\Sigma k = k_N + k_{-N} + k_O + k_{-O}$$

and

$$\Pi k = k_N(k_O + k_{-O}) + k_{-N}k_O$$

[3] No quinoidal species with $\lambda_{max}$ <468 nm have been reported for the *E. coli* tryptophan synthase system. However, we (W. F. Drewe, Jr., B. Robustell, and M. F. Dunn, unpublished results) have found that L-serine derivatives containing R–NH and R–O substituents in place of the $\beta$-hydroxyl group yield quinoidal species with $\lambda_{max}$ ranging from 452 to 468 nm.

Frank Moses, James Mason, and Carl Lentz and by Drs. Steven C. Koerber and Gene Gould at various stages in the development of our rapid kinetics systems. We also thank Dr. Edith Miles, Professor Kasper Kirschner, and Dr. Andrew Lane for stimulating discussions pertaining to these mechanism studies and for providing us with manuscripts of their work prior to publication.

## Appendix

*Comparison of This Work with the Findings of Previous Investigators.* Using fluorescence, York (1972) monitored the reaction of $\alpha_2\beta_2$ with L-serine (50 mM) and reported that the fluorescence increased within the mixing dead time (3 ms) of his instrument and then decayed via a monophasic time course with a fitted rate of 70 $s^{-1}$. Under similar conditions, we have also found that the fluorescence increases during the dead time, and our $1/\tau_2$ process has a maximum rate of 68 $s^{-1}$ (see Table I), in excellent agreement with York. Furthermore, in agreement with Lane & Kirschner (1983a), our studies establish the existence of two additional phases, $1/\tau_3$ and $1/\tau_4$ not reported by York. York's analysis of the decay time course, which was restricted to a period of 50 ms, would make difficult the observation of the $\tau_3$ process (15 $s^{-1}$ and 15% of the total amplitude change) and the $\tau_4$ process. York did report a very slow fluorescence change (similar in rate to our $\tau_4$ process) in the reaction of $\beta_2$ enzyme with L-serine. Our studies show that the absorbance changes in the wavelength region 400–468 nm (Figure 1A,C) coincide with the fluorescence changes, both in measured rates and relative amplitude changes (Table I). The absorbance changes (Figures 1 and 4) plus the fluorescence changes (Figure 5B) substantiate York's proposal that the appearance of the "pale" species ($\lambda_{max}$ = 330 nm) coincides with the disappearance of the fluorescence of the "aqua" species and the 430-nm absorbance.

Faeder & Hammes (1971) reported only one relaxation process for the $\alpha_2\beta_2$–serine reaction. They found that the rate of this process, measured at 470, 420, and 330 nm, increased hyperbolically with increasing L-serine to a maximum rate of approximately 33 $s^{-1}$. Failure by both York (1972) and Faeder & Hammes (1971) to detect the slower processes [reported both herein and by Lane & Kirschner (1983a)] can be explained as follows: The low rate constant reported by Faeder & Hammes (33 $s^{-1}$ compared to 68 $s^{-1}$) could be due to either of two causes. When our time course at 430 nm (Figure 1, trace b) is fitted with a single exponential, the rate constant obtained has a value between that of $1/\tau_2$ and $1/\tau_3$; the computer-generated "best fit" rate constant is 51 $s^{-1}$ (compared to a value for $1/\tau_2$ of 68 $s^{-1}$ when fitted assuming either two or three exponentials). Goldberg & Baldwin (1967) reported that the spectra for some $\alpha_2\beta_2$ enzyme preparations had an "abnormally" high absorbance at 330 nm, similar to the spectrum observed for an early $\alpha_2\beta_2$ preparation of ours. Using this preparation of enzyme, we observed a $1/\tau_2$ of only 38 $s^{-1}$ even when the time course was fitted to two exponentials. An interesting point can be made regarding the absorbance increase at 470 nm reported by Faeder and Hammes. According to our RSSF and single-wavelength studies, if they had chosen a wavelength in the region of 440–468 nm rather than 470 nm, then a totally different time course would have been observed (see Figure 1, trace g). The time course would have consisted of an increase followed by a decrease in absorbance, highly suggestive of the formation and decay of an intermediate.

Lane & Kirschner (1982a) followed the reaction of $\alpha_2\beta_2$ with L-serine (0.1–6 mM) by measuring the changes in fluorescence ($\lambda_{ex}$ = 405 nm, $\lambda_{em}$ > 475 nm). They found that the fluorescence increased with a single exponential ($1/\tau_1$), followed by a decay consisting of three exponential processes ($1/\tau_2$, $1/\tau_3$, $1/\tau_4$) with rates and amplitudes similar to those that characterize the absorbance changes we find at 454 nm with low L-serine (0.4 mM, Figure 1, trace g). The dependence of $1/\tau_1$ on the L-serine concentration is linear, achieving an observed pseudo-first-order rate of >400 $s^{-1}$ at 2 mM, while the dependence of $1/\tau_2$ on the L-serine concentration is hyperbolic (up to 6 mM), achieving an (extrapolated) maximum value of 47 $s^{-1}$. They reported that both $1/\tau_3$ and $1/\tau_4$ (respectively 1.6 and 0.3 $s^{-1}$) do not depend on the concentration of L-serine. They suggest that the discrepancy between their calculated maximum value for $1/\tau_2$ (47 $s^{-1}$) and York's rate constant for the fluorescence decrease (70 $s^{-1}$) is due to the activating effect of high L-serine concentrations. Evidence has been found by Heilmann & Büger (1981) from steady-state kinetic studies that L-serine exerts an activating effect at high concentrations.

We have found that both $1/\tau_2$ and $1/\tau_3$ (but not $1/\tau_4$) give hyperbolic responses as the L-serine concentration is increased (data not shown) with (extrapolated) maximum values of 68 and 15 $s^{-1}$, respectively, for $1/\tau_{2max}$ and $1/\tau_{3max}$.

York (1972) studied the reaction of the $\beta_2$ enzyme with high (5–200 mM) L-serine by following both the fluorescence of the aqua species and the increase in absorption at 430 nm. Both methods were found to give the same kinetic behavior and a fitted rate constant of 37 $s^{-1}$ (independent of concentration). York could account for only half of the fluorescence or absorbance changes by extrapolation of this reaction back to the time of mixing.

Faeder & Hammes (1970) also studied this reaction over a concentration range for L-serine of 0.5–20 mM. They reported that the absorbance at 420 and 470 nm increases, while the absorbance at 330 nm decreases with a maximum rate of 40 $s^{-1}$ (no mention of amplitudes was made). Our results partially substantiate their reported absorbance and fluorescence changes. We also find an observed rate constant of 40 $s^{-1}$ ($1/\tau_{2\beta}$) but also a faster process of 200 $s^{-1}$ ($1/\tau_{1\beta}$). It is likely that this faster process accounts for the fluorescence and absorbance changes that York could not measure. Again, the hand analyses by York of either the fluorescence or absorbance time courses would make difficult the detection of this faster process (with our dead time, the faster process accounts for only 25% of the total observed amplitude change). In the wavelength region 375–500 nm (Figure 2), the same phasicity and relative rate constants were found.

**Registry No.** PLP, 54-47-7; $D_2$, 7782-39-0; L-serine, 56-45-1; DL-serine, 302-84-1; tryptophan synthase, 9014-52-2.

## References

Adaci, O., Kohn, C. D., & Miles, E. W. (1974) *J. Biol. Chem. 249*, 7756–7763.

Becker, M. A., Kredich, N. M., & Tomkins, G. M. (1969) *J. Biol. Chem. 244*, 2418–2427.

Bernasconi, C. (1976) *Relaxation Kinetics*, pp 20–39, Academic Press, New York.

Dunn, M. F., Bernhard, S. A., Anderson, D., Copeland, A., Morris, R. G., & Rogue, J.-P. (1979) *Biochemistry 18*, 2346–2354.

Esaki, N., Tanaka, H., Miles, E. W., & Soda, K. (1983) *Agric. Biol. Chem. 47*, 2861–2864.

Faeder, E. J., & Hammes, G. G. (1970) *Biochemistry 9*, 4043–4049.

Faeder, E. J., & Hammes, G. G. (1971) *Biochemistry 10*, 1041–1045.

Goldberg, M. E., & Baldwin, R. L. (1967) *Biochemistry 6*, 2113–2119.
Goldberg, M. E., York, S., & Stryer, L. (1968) *Biochemistry 7*, 3662–3667.
Heilmann, H.-D., & Bürger, M. (1981) *Hoppe Seyler's Z. Physiol. Chem. 362*, 1567–1574.
Högberg-Raibaud, A., & Goldberg, M. E. (1977) *Biochemistry 16*, 4014–4020.
June, D. S., Suelter, C. H., & Dye, J. L. (1981a) *Biochemistry 20*, 2707–2713.
June, D. S., Suelter, C. H., & Dye, J. L. (1981b) *Biochemistry 20*, 2714–2719.
Karube, Y., & Matsushima, Y. (1976) *J. Am. Chem. Soc. 98*, 2714–2715.
Koerber, S. C. (1981) Doctoral Dissertation, University of California, Riverside, CA.
Koerber, S. C., MacGibbon, A. K. H., Dietrich, H., Zeppezauer, M., & Dunn, M. F. (1983) *Biochemistry 22*, 3424–3431.
Laemmli, U. K. (1970) *Nature (London) 227*, 680–685.
Lane, A. N., & Kirschner, K. (1981) *Eur. J. Biochem. 120*, 379–387.
Lane, A. N., & Kirschner, K. (1983a) *Eur. J. Biochem. 129*, 561–570.
Lane, A. N., & Kirschner, K. (1983b) *Eur. J. Biochem. 129*, 571–582.
Metzler, C. M., Harris, C. M., Johnson, R. J., Siano, D. B., & Thomson, J. A. (1973) *Biochemistry 12*, 5377–5392.
Metzler, C. M., Cahill, A., & Metzler, D. E. (1980) *J. Am. Chem. Soc. 102*, 6075–6082.
Miles, E. W. (1979) *Adv. Enzymol. Relat. Areas Mol. Biol. 48*, 127–186.
Miles, E. W., & McPhie, P. (1974) *J. Biol. Chem. 249*, 2852–2857.
Miles, E. W., & Moriguchi, M. (1977) *J. Biol. Chem. 252*, 6594–6599.
Miles, E. W., Hatanaka, M., & Crawford, I. P. (1968) *Biochemistry 7*, 2742–2753.
Miles, E. W., Houck, D. R., & Floss, H. G. (1982) *J. Biol. Chem. 257*, 14203–14210.
Schirch, L., & Diller, A. (1971) *J. Biol. Chem. 246*, 3961–3966.
Schnackerz, K. D., Ehrlich, J. H., Giesemann, W., & Reed, T. A. (1979) *Biochemistry 18*, 3557–3563.
Tokushige, M., Nakazaswa, A., Skizuta, Y., Okada, Y., & Hayaishi, O. (1968) in *Symposium on Pyridoxal Enzymes* (Yamada, K., Katanuma, N., & Wada, H., Eds.) p 105, Marnzen, Tokyo.
Tshopp, J., & Kirschner, K. (1980) *Biochemistry 19*, 4514–4521.
Vogel, H. J., & Bonner, D. M. (1956) *J. Biol. Chem. 218*, 97–106.
Watanabe, T., & Snell, E. E. (1977) *J. Biochem. (Tokyo) 82*, 733–745.
Yanofsky, C., & Crawford, I. P. (1970) *Enzymes (3rd Ed.) 7*, 1–31.
York, S. (1970) Doctoral Dissertation, Stanford University, Stanford, CA.
York, S. (1972) *Biochemistry 11*, 2733–2740.

# Effects of Terminal Mismatches on RNA Stability: Thermodynamics of Duplex Formation for ACCGGGp, ACCGGAp, and ACCGGCp†

David R. Hickey and Douglas H. Turner*
*Department of Chemistry, University of Rochester, Rochester, New York 14627*
*Received November 26, 1984*

ABSTRACT: The thermodynamics of ACCGGCp, ACCGGAp, and ACCGGGp helix formation have been measured in 1 M NaCl. The terminal mispairs stabilize the CCGG core duplex at $10^{-4}$ M in the order AC ≈ AA < AG ≈ AU. The data reported provide thermodynamic parameters for RNA structure prediction and suggest useful approximations for including other mismatches in current algorithms.

The importance of base mismatches in RNA interactions has become increasingly evident since the G·U wobble pair was first proposed (Crick, 1966). Mismatches are present in essentially all known and predicted RNA structures (Rich & Rajbhanday, 1976; de Brujin & Klug, 1983; Furdon et al., 1983; Noller, 1984; Dams et al., 1983; Traub & Sussman, 1982; Fox & Woese, 1975; Studnicka et al., 1981; Salser, 1977; Cech et al., 1983; Auron et al., 1982). Despite this prevalence, contributions of mismatches have been largely ignored in predictions of RNA stability due to lack of measured parameters (Tinoco et al., 1971; Borer et al., 1974; Salser, 1977; Zuker & Stiegler, 1981). Nevertheless, there is evidence mismatches add significant stability to double helices (Alkema et al., 1981). Previous attempts to incorporate such effects have been based on indirect estimates of the thermodynamic parameters for mismatches (Papanicolaou et al., 1984). This paper reports thermodynamic parameters for duplex formation by ACCGGGp, ACCGGAp, and ACCGGCp. Comparison with previous results for CCGG (Petersheim & Turner, 1983) provides parameters for AG, AA, and AC terminal mismatches.

## Materials and Methods

*Oligonucleotide Synthesis.* ACCGGXp's (X = A, C, or G) were synthesized by successive addition of nucleoside

† This work was supported by National Institutes of Health Grant GM 22939.

0006-2960/85/0424-3987$01.50/0 